Effect of Fe(II)/Fe(III) species, pH, irradiance and bacterial presence on viral inactivation in wastewater by the photo-Fenton process: Kinetic modeling and mechanistic interpretation

Stefanos Giannakis [a,*], Siting Liu [a], Anna Carratalà [b], Sami Rtimi [a], Michaël Bensimon [c], César Pulgarin [a,**]

[a] SB, ISIC, Group of Advanced Oxidation Processes (GPAO), École Polytechnique Fédérale de Lausanne (EPFL), Station 6, CH-1015, Lausanne, Switzerland
[b] ENAC, IIE, Laboratory of Environmental Chemistry (LCE), École Polytechnique Fédérale de Lausanne (EPFL), Station 2, CH-1015, Lausanne, Switzerland
[c] ENAC, IIE, Central Environmental Laboratory (CEL), Ecole Polytechnique Fédérale de Lausanne (EPFL), Station 18, 1015, Lausanne, Switzerland

ARTICLE INFO

ABSTRACT

Advanced Oxidation Processes and in particular photo-Fenton, represent promising strategies of pathogen inactivation in wastewater effluents. Nevertheless, its full potential is not yet unlocked, as the efficacy of photo-Fenton against viruses has not been deeply explored. In this work, we characterize the effect of major parameters (Fe species and concentration, solar irradiance, pH and microbial competition) on the inactivation of MS2 Coliphage by the photo-Fenton process. The use of Fe(II) salts, under any combination of H_2O_2 concentration, sunlight irradiance or starting pH (6–8), induced a faster inactivation compared to their Fe(III) counterparts. Moreover, ICP-MS analyses revealed that starting with Fe(II) resulted to higher amount of iron in solution longer than Fe(III), which led to higher inactivation kinetics. Even so, a 4-log MS2 inactivation was achieved upon exposure to $600 \, W/m^2$ for 30 min in presence of Fe(III) and H_2O_2 (1:1 ratio). Furthermore, the inactivation of MS2 was only slightly decreased in presence of the bacterial host, suggesting a low competition for the oxidants in the bulk. The enhancement of iron solubilization through its complexation by organic matter present in wastewater was also investigated, observing an efficient viral inactivation despite the presence of reactive oxygen species (ROS) scavengers. The present data have been used to propose a simple model describing MS2 photo-Fenton inactivation in wastewater. Finally, the pathway describing the photo-Fenton-induced MS2 inactivation in wastewater was proposed, in presence or absence of bacteria.

© 2016 Elsevier B.V. All rights reserved.

1. Introduction

Wastewater disinfection is of major importance to prevent the microbial contamination of downstream water resources. Treatment strategies such as filtration, chlorination or UV-radiation for microbial inactivation have been developed over the last decades and their efficiency against bacteria [1], viruses [2,3] and parasites [4,5] has been assessed in a number of studies. Nevertheless, treatment strategies are turning towards greener and more sustainable techniques, such as the Advanced Oxidation Processes (AOPs).

Among these techniques, the photo-Fenton process has emerged as a prominent solution to treat chemical contaminants [6], but the number of studies focusing on microorganisms is significantly inferior. This process has been found to inactivate structurally simple [7], complex [8] or resistant microorganisms [9], and is promoted because of its simplicity, low cost and limited environmental footprint [10]. In the Fenton reaction, hydrogen peroxide reacts with iron generating hydroxyl radicals, which are the predominant reactive oxidizing species (ROS) responsible for microorganism inactivation in AOPs, and effectively oxidize microbial components, such as amino acids and nucleotides [11,12]. In this process, iron acts as a catalyst, is repeatedly oxidized and reduced. In wastewater, the process becomes significantly more complicated, due to the chemical and biological complexity of the matrix and the imminent iron precipitation due to the near-neutral pH (6–8). Also, the presence of effluent organic matter (EfOM) in wastewater (e.g. humic acid, fulvic acid), can scavenge a significant part of the generated HO•, leading to a weakened inactivation [13]. However, other reports have pointed out that light radiation

* Corresponding author.
** Corresponding author.
E-mail addresses: stefanos.giannakis@epfl.ch (S. Giannakis), cesar.pulgarin@epfl.ch (C. Pulgarin).

on EfOM components (i.e. the dissolved fraction of the organic matter, DOM) can create intermediate radical species, which react with water to generate HO• [14], and partially compensate for the loss of HO• by DOM.

Furthermore, Fe ions form complexes with organic matter and these Fe-organo species not only absorb light, but also stabilize at near neutral pH. This extends the application of the homogenous photo-Fenton reaction with less pH dependency [15]. Under solar light exposure, the organic ligands that compose the DOM form complexes with Fe(III) and participate in a ligand-to-metal charge transfer (LMCT) type reaction [16]. However, during the photo-Fenton process, both organics degradation and microorganism inactivation would compete. DOM may scavenge ROS and provide targets of degradation with protection sites [17].

Most of the previous works on the efficacy of photo-Fenton processes against microorganisms at near neutral-pH were done targeting bacteria (e.g. [18–22]), either in pure water or simulated wastewater with NOM-like substances. To date, however, there is much less experimental information on the efficiency and parameters governing the photo-Fenton inactivation of viruses [7,14,23–25]. MS2 bacteriophage is a single-stranded RNA virus, which infects *Escherichia coli* thorough the pili and resembles certain human enteric viruses in size (27.5 nm) and structural complexity. Also, it can be rapidly cultivated in laboratory conditions up to the high concentrations needed for most inactivation studies, is easily purified, not pathogenic to humans [26,27], which explains its frequent selection as a model virus in microorganism inactivation studies [28].

The main purpose of this work is to assess the overall efficiency of photo-Fenton inactivation against viruses in wastewater, using MS2 bacteriophage as a model. Furthermore, the effect of major parameters implicated in the process (namely Fe species and concentration, sunlight irradiance, initial pH and bacterial competition for ROS) is also assessed, emphasizing the alterations inflicted by the presence of organic matter in the matrix. The obtained datasets were used to propose a mathematical and a mechanistic model to describe the pathways exerted during the photo-Fenton inactivation of MS2 bacteriophage in wastewater.

2. Materials and methods

2.1. Chemicals and reagents

In the experiments, all the chemicals were reagent grade or above, and all the solutions were prepared in water purified at analytical grade using a Millipore Elix 3 system combined with a Progard filter (Millipore AG, Zug, Switzerland). The pH measurement was handled by a digital pH-meter (S220 SevenCompact^{TM} pH/Ion, Mettler Toledo, Griefensee, Switzerland).

2.1.1. Fenton reagents

Iron salts of $FeSO_4 \cdot 7H_2O$ (≥99.0%, Sigma-Aldrich) or $Fe_2(SO_4)_3 \cdot xH_2O$, (97%, Sigma-Aldrich, Buchs, Switzerland) were used according to the required starting iron species. The H_2O_2 stock solution in water was prepared with Perdrogen^{TM} (H_2O_2, 30% w/w, refrigerated, Sigma-Aldrich, Buchs, Switzerland) and the quenching agent for H_2O_2 residuals was aqueous solution prepared with a mixture of $NaHSO_3$ and $Na_2S_2O_5$, (99% Acros Organics, Basel, Switzerland).

2.1.2. Synthetic secondary wastewater

The synthetic wastewater was chosen rather than the secondary effluent from WWTP, for its ability to provide an identical water matrix for every single experiment. The composition of the synthetic secondary wastewater is shown in Table 1 [29]. A concentrated stock solution (×10 times) was prepared every week, kept at

4 °C and dilution to reach the levels of Table 1 was done every day. The dilution was regulated to neutral pH (pH 6, 7 or 8 in different series of experiment with 0.1 M NaOH or HNO_3) before use.

2.1.3. Fe(II)/Fe(III) determination

The Fe(II)/Fe(III) concentrations in experimental samples were measured by a modified Ferrozine method [30], in which Fe ions chelated with the organic ligand Ferrozine and the formed magenta iron complex was determined by absorbance measurement at 562 nm. This modified method could be applied to detect μM level of Fe ions in water samples containing DOM. Inductively coupled plasma mass spectrometry (ICP-MS) was also used to monitor trace Fe amounts during experiments. The Finnigan^{TM} ICP-MS 7-238-NU1700 (Nu Instruments, Wrexham, UK) used was equipped with a double focusing reverse geometry mass spectrometer presenting low background signal and high ion-transmission coefficient. The spectral signal resolution was 1.2×10^5 cps/ppb. Fe from the solutions was digested in 69% nitric acid (1:1 ratio HNO_3:H_2O), ensuring organics removal in solution and ions adhesion to the vial wall. MS quantification of Fe concluded the analyses.

2.1.4. H_2O_2 determination

During the photo-Fenton experiments, the H_2O_2 concentration in the system was monitored. By reacting with 10 μL of titanium(IV) oxysulfate solution ($TiOSO_4$, 1.9-2.1%, Sigma-Aldrich, Buchs, Switzerland), the H_2O_2 concentration in a 1 mL experimental sample was quantified by measuring the colorimetric absorbance of the produced yellow-colored pertitanic acid (H_2TiO_4) at 410 nm [31].

2.2. Sunlight source and reactors

2.2.1. Suntest solar simulator

The experiments were conducted using a solar simulator (CPS Suntest System Heraeus Noblelight, Hanau, Germany) with infrared and UVC cut-off filters in order to simulate solar global radiation from outdoor daylight and to prevent from the influence of UVC radiation and thermal heating (the emitted spectrum can be found in the Supplementary material). The solar radiation intensities used in the assays were 300, 600 and 900 W/m^2 (global irradiance) which were monitored by the combination of a UV radiometer and a pyranometer connected to a data-logger (CUV3 and CM6b respectively, Kipp & Zonen, Delft, Holland). These values represent typical intensities achieved by solar light for different seasons, latitude and/or time points within a day. According to previous experiments and own current measurements performed under the same conditions, the temperature in the simulator never exceeded 38 °C [15].

An irradiance of 300 W/m^2 was selected in the experiments concerning pH variations and different ratios of Fenton reagents. At this relatively low light intensity, the MS2 inactivation was slower and the inactivation kinetics could be better distinguished. However, the inactivation experiments in systems of MS2 and host *E. coli* coexistence were carried out under the irradiance of 600 W/m^2 in order to enhance the *E. coli* inactivation rates.

2.2.2. Glass reactors

All the solar radiation experiments were performed in Pyrex, UVB-transparent glass vials of 100 mL, while brown ones were used in the dark Fenton controls. Inside the solar simulator, a rectangular stirrer (MIX 15 eco, 2Mag Magnetic Motion, München, Germany) was used to place the reactors and the reaction solutions were continuously stirred at 350 rpm. In order to avoid iron cross-contamination, after every set of experiments, all glass reactors were soaked in 10% HNO_3 overnight and then rinsed with deionized water before heat-sterilization.

Table 1
Composition of synthetic secondary wastewater [28].

Substances	Composition [mg/L]
Meat extract (Sigma-Aldrich)	1.8
Peptone from meat, peptic digest (Sigma-Aldrich)	2.7
Humic acid (Carl Roth)	4.25
Tannic acid (AppliChem)	4.18
Lignosulfonic acid, sugared sodium salt (Sigma-Aldrich)	2.4
Sodium dodecylsulfate ($NaC_{12}H_{25}SO_4$, 98%, Abcr)	0.9
Arabic gum powder (Acros Organics)	4.7
Ammonium sulfate (($NH_4)_2SO_4$, ≥99.0%, Carlo Erba Reagents)	7.1
Potassium phosphate dibasic (K_2HPO_4, ≥99.0%, Sigma-Aldrich)	7
Ammonium bicarbonate (NH_4HCO_3, ≥99.0%, Sigma-Aldrich)	19.8
Magnesium sulfate heptahydrate ($MgSO_4 \cdot 7H_2O$, Sigma-Aldrich)	0.71

2.3. Microorganisms and quantification methods

2.3.1. Microorganisms

MS2 phage (DSMZ 13767) and the antibiotic-resistant (2 mg/L streptomycin) strain of bacterial host *Escherichia coli* (DSMZ 5695) were obtained from Deutsche Sammlung von Mikroorganismen und Zellkulturen (DSMZ, German Collection for Microorganisms and Cell Cultures, Braunschweig, Germany).

The propagation and purification of the coliphage was following the procedure described by Ortega-Gómez et al. [25]. The preparation of the bacteria for the co-culture experiments followed a protocol similar to the one for *E. coli* K-12 [32,33].

2.3.2. Phage and bacteria quantification

Infective MS2 Coliphage was measured by the double agar layer technique (DAL, EPA Method 1602, 2001). Plates were incubated at 37 °C for 18–24 h in a CO_2-controlling incubator (B 5060 EK-CO2, Heraeus Instruments, Hanau, Germany) and then the plaque forming units (PFU) were counted manually. The detection limit of these experimental methods was found to be 10 PFU/mL. *E. coli* were handled with the spread plate technique and colonies were quantified by the standard plate count method and results were collected similarly.

2.4. Inactivation experiments

At the beginning of each experiment, 50 mL of the spiked wastewater matrix in the glass reactor was stirred in the dark for 10 min to get evenly mixed. By adding 50 μL of 10^9 PFU/mL MS2 stock in carbonate buffer solution (CBS, 8.401 mg $NaHCO_3$, Sigma-Aldrich, and 876.6 mg NaCl, Sigma-Aldrich, dissolved in 1000 mL of water, adjusted to pH 8), the initial concentration of infective MS2 was around 10^6 PFU mL^{-1}. The reactors were then spiked with Fe(II)/(III) from freshly prepared stock solutions (500 mg/L) to reach the final concentration at 0.25, 0.5 or 1 mg/L. Lastly, H_2O_2 was added from a fresh stock solution (1000 mg/L) and the final concentration was 0.5 or 1 mg/L. Next, the Xenon lamp was turned on to photo-inactivate viruses under continuous irradiation at constant intensity. Corresponding control experiments containing MS2 and Fe ion or H_2O_2 alone, under solar light or in the dark, were also conducted. To monitor MS2 inactivation in the presence of its host, experiments were conducted at the light intensity of 600 W/m^2, using 1 mg/L of Fe and 1 mg/L of H_2O_2.

During the experimental process, samples of 0.5 mL were taken at certain time intervals and immediately mixed with 10 μL $NaHSO_3$ aqueous solution (100 mg/L) to scavenge exceeding H_2O_2. Inactivation of MS2 and *E. coli* caused by $NaHSO_3$ and dilution solutions was negligible over the experimental period [7]. Finally, before use, all the materials and solutions were autoclaved at 15 psi, 121 °C for 15 min (Fedegari FVG1, Vitaris AG, Baar, Switzerland) to achieve complete sterilization.

2.5. Data treatment and analysis

Experimental data were expressed as the measured plaque forming units over time (PFU/mL vs. time), where the instant MS2 concentrations were presented as arithmetic means ± standard deviations calculated from the last three serial sample dilutions. For experiments involving host *E. coli*, the same operation was done in interpreting its colony forming units (CFU/mL).

From the slope of a linear regression of ln([virus]/[virus]$_0$) vs. time, the observed k was determined as the first-order inactivation rate in each individual experiment. In the systems involving Fe(II), where the inactivation was better approximated by a two-phase exponential approach [7], for each phase a first-order k_{obs} was determined. The curve fitting for each series of experiment was conducted with Maple 18 (Waterloo Maple Inc., Waterloo, Canada) or Microsoft Excel 2010 (Microsoft Corp., Redmond, Washington, USA).

3. Results and discussion

3.1. Isolated effect of the photo-Fenton constituents

First and foremost, all the experiments conducted in this work took place in a (simulated) secondary wastewater matrix, therefore the inherent challenges encountered when stepwise constructing the photo-Fenton process merit a separate mention.

3.1.1. Effect of the Fenton reagents in absence of light and the effect of solar irradiance

MS2 infectivity was well preserved in absence of light and Fenton reagents' addition (see Supplementary Fig. 1). These results were similar to the viral survival curve obtained in CBS [25], although here at pH 7 and a complex dilution matrix. Adding 0.25 mg/L of Fe(II), Fe(III) or 0.5 mg/L of H_2O_2 had a negligible effect within 60 min (<0.5-log inactivation). When both Fe ion and H_2O_2 were applied simultaneously, the (dark) Fenton system with Fe(II) showed a 1.2-log inactivation while almost no virucidal effect was observed for the Fe(III) system; this differentiation is also parallel (but lower) to Kim et al. [7], where CBS served as the MS2 suspension medium. Although 1.2-log inactivation is low, the higher efficiency compared to the other (milder or Fe(III)-driven) processes reveals the potential of viral infectivity decrease in the complex WW matrix.

When samples were exposed to (global) irradiance of 300, 600 or 900 W/m^2 for 60 min, the infectivity of MS2 did not demonstrate a significant decrease, which indicated the relatively high resistance of MS2 towards UV/visible light, in accordance to previous findings [24,25]. In addition, the wastewater matrix itself did not show a notable impact on virus inactivation under solar radiation. The operating pH (initial pH:7) and the presence of particles did

not significantly affect the infectivity of the viruses present in the matrix.

3.1.2. Effect of H_2O_2 or Fe addition on MS2 sunlight inactivation

In Fig. 1a, under 600 W/m² of solar irradiance, H_2O_2 doses of 0.5 and 1 mg/L contribute at about 0.5 log MS2 inactivation further than the effect of solar radiation alone. This result contradicts what was reported by Ortega-Gómez et al. [25] in buffered water, which showed a total inactivation after 50 min by 1 mg/L of H_2O_2. The virucidal effect was explained as a consequence of solar irradiation that made MS2 more sensitive to oxidants, rather than the impact of HO• itself [25]. The apparent contradiction of low H_2O_2 efficiency here, however, could be interpreted by the presence of NOM-like substances in the specific water matrix, which can act as efficient scavengers of HO• [34] and non-selectively react with H_2O_2 in competition with MS2 particles.

As shown in Fig. 1b, dissolved Fe ions in wastewater induced a more effective MS2 inactivation than hydrogen peroxide under solar irradiation. The addition of 0.5 mg/L of Fe(II) resulted in a decay of 2.9-log, while in the presence of 1 mg/L MS2 inactivation reached 3.5 log units. For Fe(III), the amount of 0.5 mg/L had a decrease by 1.8 logs, and 1 mg/L led a 2.5-log inactivation. Nieto-Juarez et al. [24] observed that MS2 infectivity dropped by half over 30 min in their CBS matrix containing 0.056 mg/L of Fe(III), and considered this degradation as either virus inactivation by Fe ion alone or virus aggregation. The possibility of spontaneous aggregation of MS2 is unlikely here, as Fe-induced MS2 removal by excessive aggregation was found negligible by filtering samples prior to plating as well (0.2 μm filtering) and comparing the results with un-filtered ones (data not shown). Thus, it is implied that Fe ions serve as the main actors of inactivation in the Fe/light system.

According to previous works concerning virus-metal interaction, the LMCT process would occur in the iron- and MS2-spiked water matrix, where the iron-MS2 "complex" acted as a light sensitizer [25]. These iron-MS2 complexes resulted from the interaction of Fe cations and negatively-charged MS2 virions (pI = 3.9) in the wastewater. However, in our experiments, the observation that Fe(II) contributed to a higher MS2 inactivation than Fe(III) in wastewater contradicts the aforementioned results, and implies an efficient electron transfer from iron first, most probably a direct reduction of viral capsid elements with oxidation of Fe(II) to Fe(III). Afterwards, the events in the two iron systems follow the same catalytic cycle. Nevertheless, the enhanced inactivation events observed, despite the scavenging effects of DOM, suggest complexation possibilities of iron in this matrix, and higher participation in MS2 inactivation than in the buffered waters [7,25], and called for further experimentation.
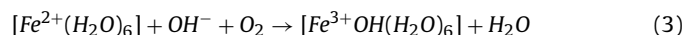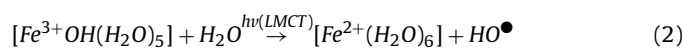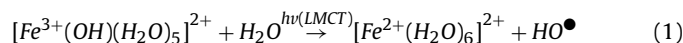
3.2. Parametrization of MS2 inactivation by the photo-Fenton process in wastewater

The following section summarizes the experimental assays combining the main actors in wastewater disinfection by the photo-Fenton reaction, namely irradiance, Fe:H_2O_2 ratio, Fe starting species and initial pH.

3.2.1. Effect of solar irradiance and Fe species

Fig. 2 shows that solar light significantly enhanced the virucidal effect of Fenton reaction. For Fe(II) (Fig. 2a), at pH 7 and initial concentrations as low as 0.5 mg/L Fe(II) and 1 mg/L H_2O_2, an increasing sunlight irradiance caused a dramatic decay of MS2 titers (3-log) as compared to the inactivation observed in the dark, reaching the detection limit (DL) after a 6-log decay in 10 min. In the Fe(III)-involving system (Fig. 2b), only an irradiance of 900 W/m² could achieve the same extent of inactivation after an exposure during 60 min, while exposure at 300 W/m² and 600 W/m² still improved
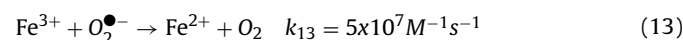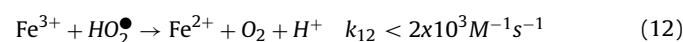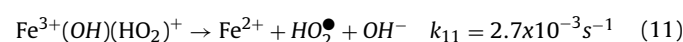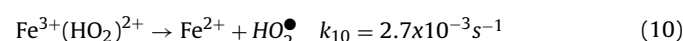
MS2 inactivation by 2.4 and 3 log, compared to the Fenton process alone, respectively. The dependence of inactivation efficiency on light intensity in presence of Fe(III) implies a photonic limitation of the system and dependence of the solar-driven actions in order to achieve viral inactivation. This effect suggests that while the Fe(II) photo-assisted process is not light intensity-dependent, it has a direct HO•-related inactivation, but for Fe(III), the Fe(III) complexes with WW are photo-active and the light-assisted LMCT process is the driving force of the inactivation process (Eqs. (1)–(3)) [11,12]:
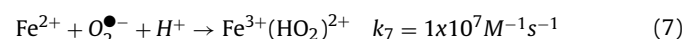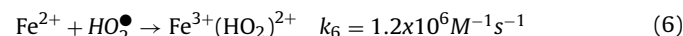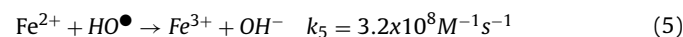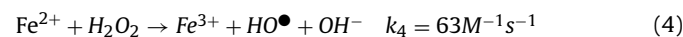
$$[Fe^{3+}(OH)(H_2O)_5]^{2+} + H_2O \overset{h\nu(LMCT)}{\rightarrow} [Fe^{2+}(H_2O)_6]^{2+} + HO^\bullet \quad (1)$$

$$[Fe^{3+}OH(H_2O)_5] + H_2O \overset{h\nu(LMCT)}{\rightarrow} [Fe^{2+}(H_2O)_6] + HO^\bullet \quad (2)$$

$$[Fe^{2+}(H_2O)_6] + OH^- + O_2 \rightarrow [Fe^{3+}OH(H_2O)_6] + H_2O \quad (3)$$

3.2.2. Effect of Fe:H_2O_2 ratio and Fe starting species

Increasing the initial concentration of Fe ions in the experimental water matrix led to an improved MS2 inactivation effect in both Fe(II) and Fe(III) starting form (Fig. 3a and b, respectively). Using Fe(II) at low concentrations (0.25:0.5) at pH = 7 required 30 min for total inactivation and after doubling, the necessary time reached the 2′ experimental limitation (minimum time from sampling to plating). On the contrary, only the high ratios, employing 1 mg/L of Fe(III) and 1 mg/L of H_2O_2 under 300 W/m² of sunlight, 6-log inactivation was achieved, in 50 min. In the meantime, lower concentrations of Fe(III) (0.25 mg/L and 0.5 mg/L) ended in only 1- and 2.2-log inactivation. The inactivation rate showed a dependency on the initial Fe concentration, as well as verifying the dependence of the starting iron species. Ortega-Gómez et al. [25] interpreted that the formation of Fe-MS2 complex was favored by the increasing amount of Fe ion, resulting in the generation of oxidants close to virus particles, crucial for their efficient inactivation [24].

The variation of inactivation effects by different initial concentrations of H_2O_2 was also displayed in Fig. 3a and b. In sunlit Fe(III) (0.25 mg/L) systems, 1 mg/L of H_2O_2 increased the proportion of inactivated MS2 by 0.5 log, when compared with the employment of 0.5 mg/L. When reacting with 0.25 mg/L of Fe(II), by applying more H_2O_2, time used to reach complete inactivation was shortened from 30 min to 15 min. Clearly, the difference due to varied H_2O_2 concentrations exhibited in a second phase (after 2 min) of inactivation. As mentioned before, since the second period was driven by the regeneration of Fe(II) from Fe(III), a higher concentration of H_2O_2 helps accelerate the overall inactivation process by the produced ROS (Eqs. (4)–(13)) [11,12].

$$Fe^{2+} + H_2O_2 \rightarrow Fe^{3+} + HO^\bullet + OH^- \quad k_4 = 63 M^{-1}s^{-1} \quad (4)$$

$$Fe^{2+} + HO^\bullet \rightarrow Fe^{3+} + OH^- \quad k_5 = 3.2x10^8 M^{-1}s^{-1} \quad (5)$$

$$Fe^{2+} + HO_2^\bullet \rightarrow Fe^{3+}(HO_2)^{2+} \quad k_6 = 1.2x10^6 M^{-1}s^{-1} \quad (6)$$

$$Fe^{2+} + O_2^{\bullet-} + H^+ \rightarrow Fe^{3+}(HO_2)^{2+} \quad k_7 = 1x10^7 M^{-1}s^{-1} \quad (7)$$

$$Fe^{3+} + H_2O_2 \leftrightarrow Fe^{3+}(HO_2)^{2+} + H^+ \quad kI_8 = 3.1x10^{-3} \quad (8)$$

$$Fe(OH)^{2+} + H_2O_2 \leftrightarrow Fe^{3+}(OH)(HO_2)^+ + H^+ \quad kI_9 = 2x10^{-4} \quad (9)$$

$$Fe^{3+}(HO_2)^{2+} \rightarrow Fe^{2+} + HO_2^\bullet \quad k_{10} = 2.7x10^{-3}s^{-1} \quad (10)$$

$$Fe^{3+}(OH)(HO_2)^+ \rightarrow Fe^{2+} + HO_2^\bullet + OH^- \quad k_{11} = 2.7x10^{-3}s^{-1} \quad (11)$$

$$Fe^{3+} + HO_2^\bullet \rightarrow Fe^{2+} + O_2 + H^+ \quad k_{12} < 2x10^3 M^{-1}s^{-1} \quad (12)$$

$$Fe^{3+} + O_2^{\bullet-} \rightarrow Fe^{2+} + O_2 \quad k_{13} = 5x10^7 M^{-1}s^{-1} \quad (13)$$
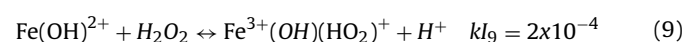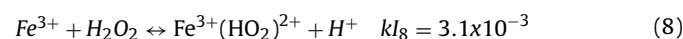
Because of the interaction between Fe(II)/Fe(III) and negatively-charged DOM (e.g. the pI of humic acid is around 2) [14], H_2O_2 was more efficiently used in the inactivation by photo-Fenton process
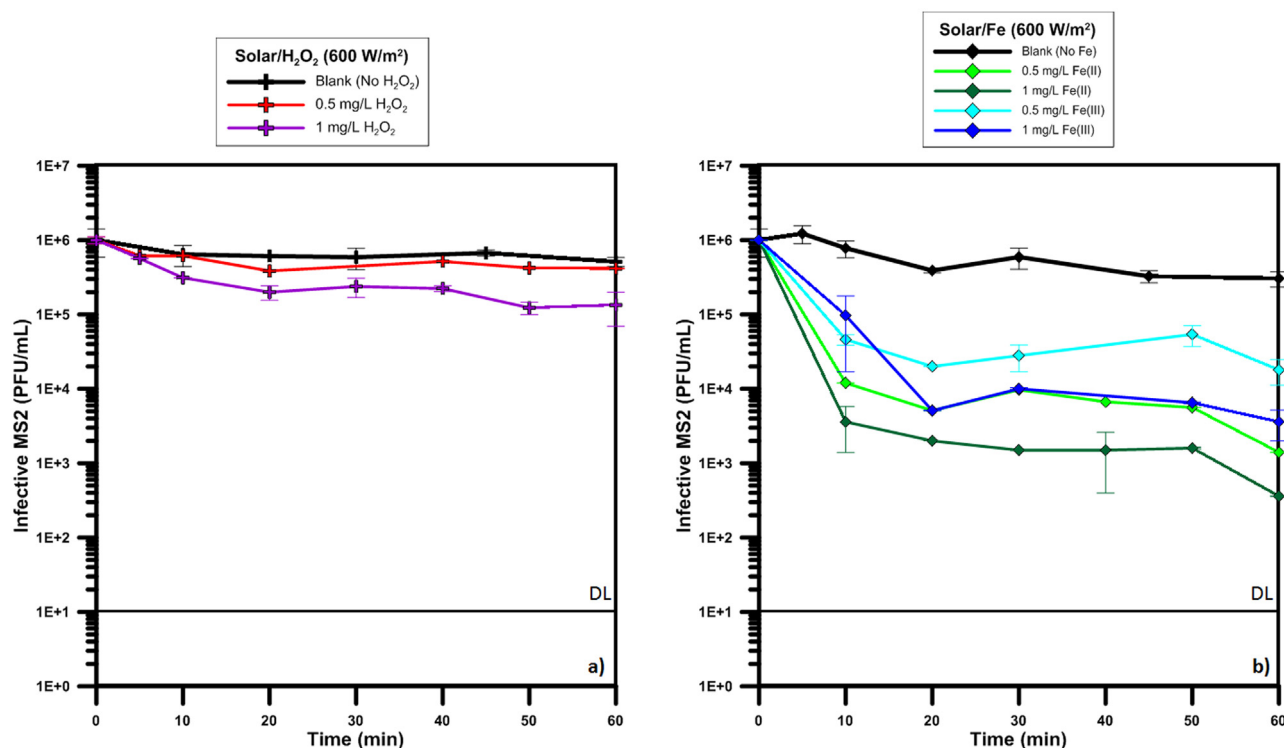
Fig. 1. Solar/H_2O_2 and Solar/Fe control experiments. a) Isolated effect of the operating H_2O_2 levels of this work. b) Addition of 0.5 or 1 mg/L Fe(II) or Fe(III) salts. DL: detection limit.
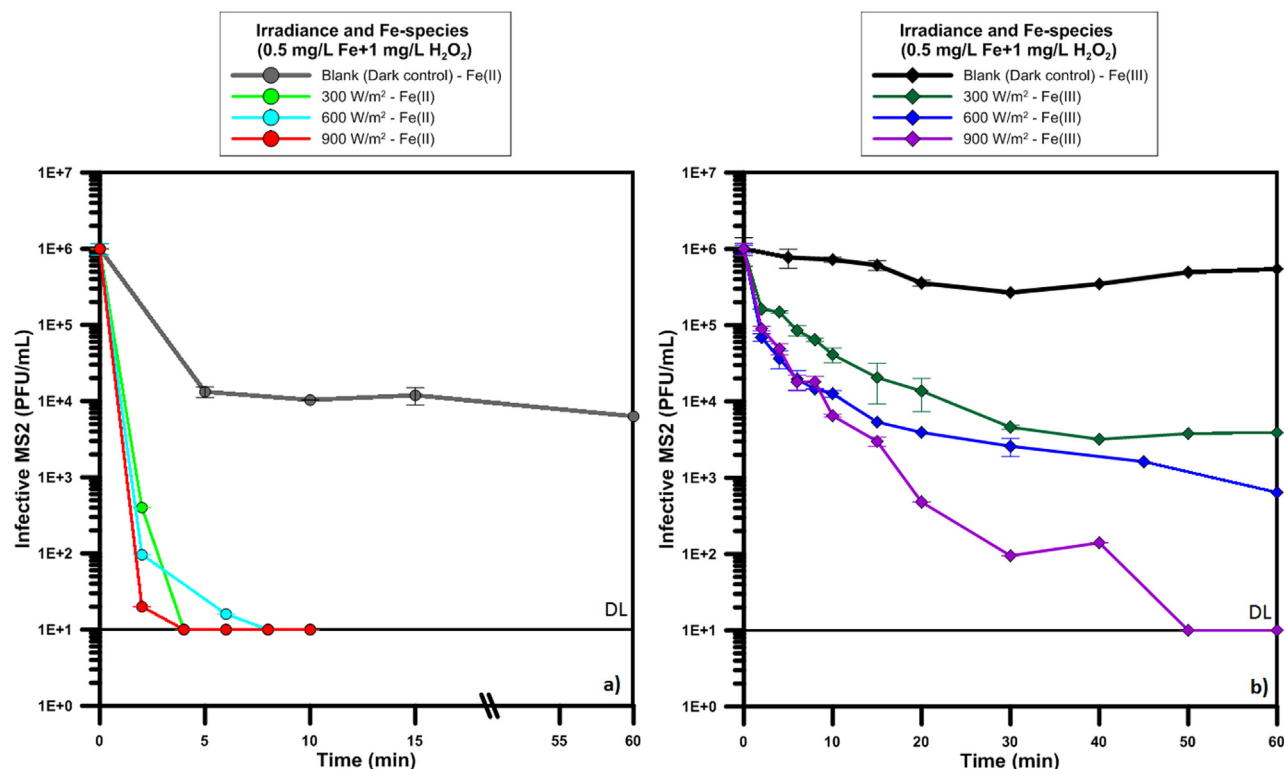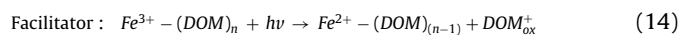

Fig. 2. Effect of solar irradiance on the evolution of MS2 inactivation by the photo-Fenton reaction. A) Fe(II) as starting iron species. B) Fe(III) as starting iron species. A notable difference exists in the kinetics of Fe(II) or Fe(III) experiments. DL: detection limit.

with Fe-DOM complexes than having its ROS quenched by it (Eqs. (14)-(15)) [11,12].

$$\text{Facilitator}: \quad Fe^{3+} - (DOM)_n + h\nu \rightarrow Fe^{2+} - (DOM)_{(n-1)} + DOM_{ox}^+ \quad (14)$$

$$\text{Antagonist}: \quad DOM + HO^\bullet \rightarrow DOM_{ox}^+ + OH^- \quad (15)$$

This explanation might be confirmed by the colorimetric H_2O_2 measurements during the experiments, where the concentrations
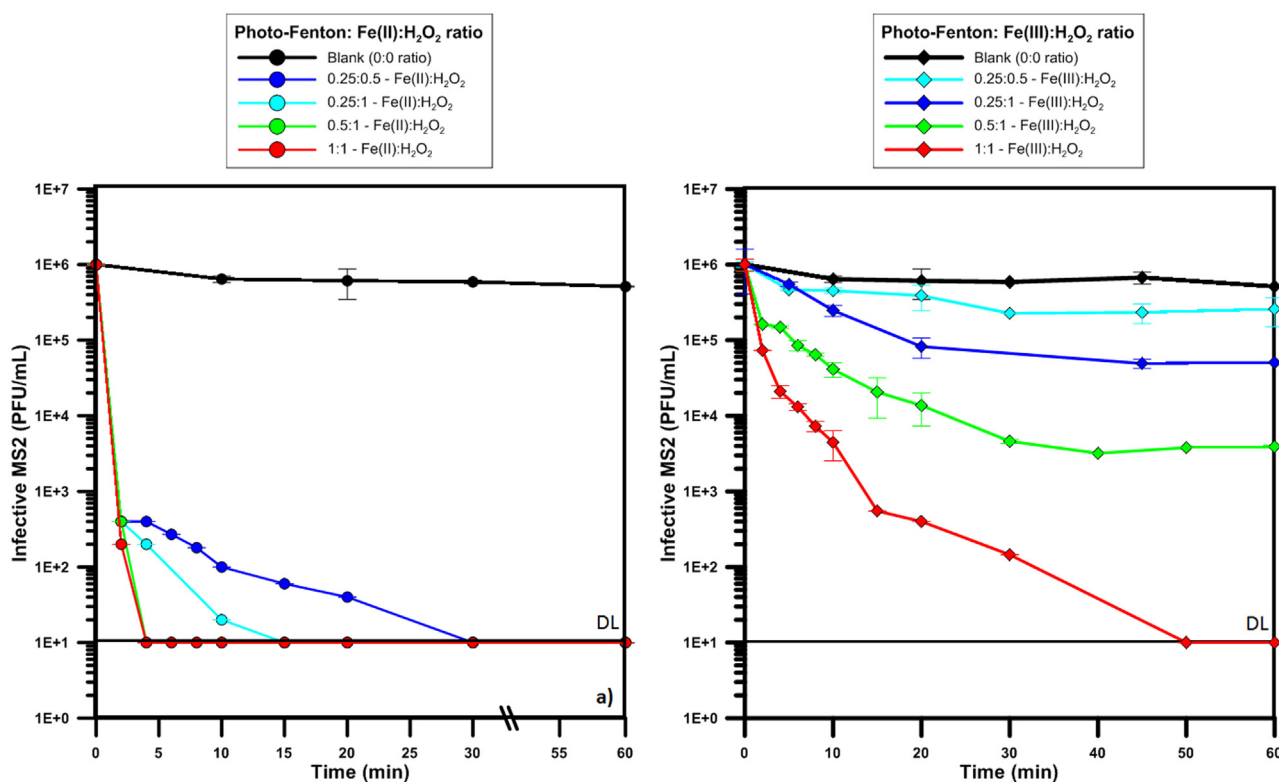
Fig. 3. Effect of the Fe:H_2O_2 ratio on the evolution of MS2 inactivation by the photo-Fenton process (light intensity: 300 W/m^2). a) Fe(II) as starting species. b) Fe(III) as starting species.

of H_2O_2 in the system can be considered constant (data not shown). Our findings agree with [35] who assumed that H_2O_2 was constantly regenerated by $HO_2^{\bullet}$ and $HO^{\bullet}$ radical reactions, through the following scheme [11,12]:

$$Fe^{2+} + O_2^{\bullet -} \rightarrow Fe^{3+} + H_2O_2 \qquad (16)$$

Fig. 3 shows that the MS2 survival curves in photo-Fenton systems containing Fe(II) or Fe(III) have different shapes. The Fe(II)-induced photocatalysis demonstrated a sudden decrease and all viruses were inactivated in 5 min; comparing to the curve of 0.25 mg/L of Fe(II) and 0.5 mg/L of H_2O_2, which showed a distinction of two inactivation phases, the proposal is that although the Fe(II) performance includes two distinct phases, due to its relatively high ability of disinfection, the second phase was only observed as a tailing pattern under low concentrations (<0.5 mg/L). Tailing in UV-inactivation studies has been attributed to recombination of viruses [36] which requires that multiple (inactivated) MS2 virions to infect the same host cell [37]. However, the onset of a tailing in MS2 decay was not observed for Fe(III). In this case, the overall inactivation rate was lower, and the decrease of MS2 infectivity followed a logarithmic curve without phase distinction. At a ferric dose of 0.5 mg/L, it was not able to inactivate MS2 beyond 2.5 logs in 60 min. The second phase in the Fe(II) system at low concentrations is correlated with the dependence to the Fe(III) presence, whose inactivation kinetics are slower.

3.2.3. Effect of the starting pH

The influence of pH on the photo-Fenton system is shown in Fig. 4. The pH of applied water matrices was measured before and after each experiment, with negligible drop noticed after 60 min of experimental time. Although all the experiments were handled at near neutral pH, the variation of the starting pH from 6 to 8 created a remarkable difference between inactivation rates. In photo-Fenton experiments driven by Fe(II), when pH was 6 or 7, a complete inac-

tivation was achieved in less than 5 min; at pH 8, in 60 min the inactivation of MS2 was no more than 3.5 logs. When the starting Fe ion was trivalent, the results of pH 6 and 7 were even more different. At pH 6, viruses were all inactivated in 10 min, at pH 7, the inactivation was completed in 50 min at a ferric dose of 1 mg/L and a pH of 8 did not favor the photo-Fenton reaction, with inactivation of 0.8 log being attained.

3.3. Effect of bacterial competition on MS2 inactivation in wastewater

The experiments mentioned until now were all performed in sterile synthetic wastewater spiked only with MS2. Normally in wastewater, a number of different microorganisms (bacteriophages, their bacterial hosts and other microorganisms) co-exist and may play an important role in each other's life cycle; certain bacteria can grow and reproduce in the environment, while virus are capable of infecting them. To verify if the proposed conditions of the photo-Fenton reaction could also apply to a more realistic situation in which different microorganisms coexist, experiments were conducted in reactors simultaneously spiked with MS2 bacteriophage and its bacterial host E. coli (Fig. 5). Since no significant increase of MS2 titers was observed during the course of these experiments the effect of phage infection to the host could be ignored.

When E. coli alone were exposed to the treatment conditions (Fig. 5a) at which we achieved total MS2 inactivation (1:1 ratios in mg/L and 600 W/m^2 solar intensity), the viability of E. coli slightly dropped in 60 min, comparing to a 0.5-log decrease when MS2 was present (Fig. 5b). Naturally, viruses consume oxidants in competition with bacteria. However, since a virion is one or two orders of magnitude smaller than a bacterium and has a simpler structure, in the photocatalytic system an identical amount of generated ROS could kill more individual viruses, while E. coli inactivation
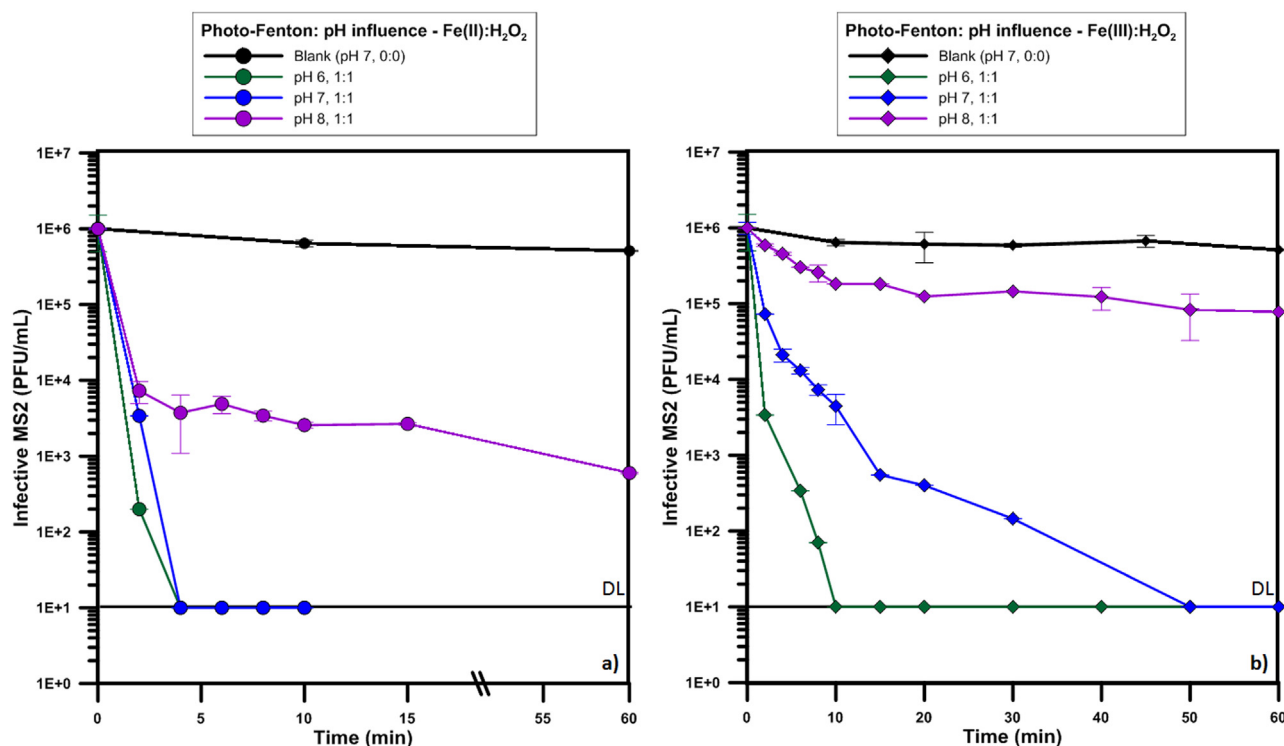
Fig. 4. Effect of the starting pH on the evolution of MS2 inactivation by the photo-Fenton process (light intensity: 300 W/m^2). a) Fe(II) as starting species. b) Fe(III) as starting species.
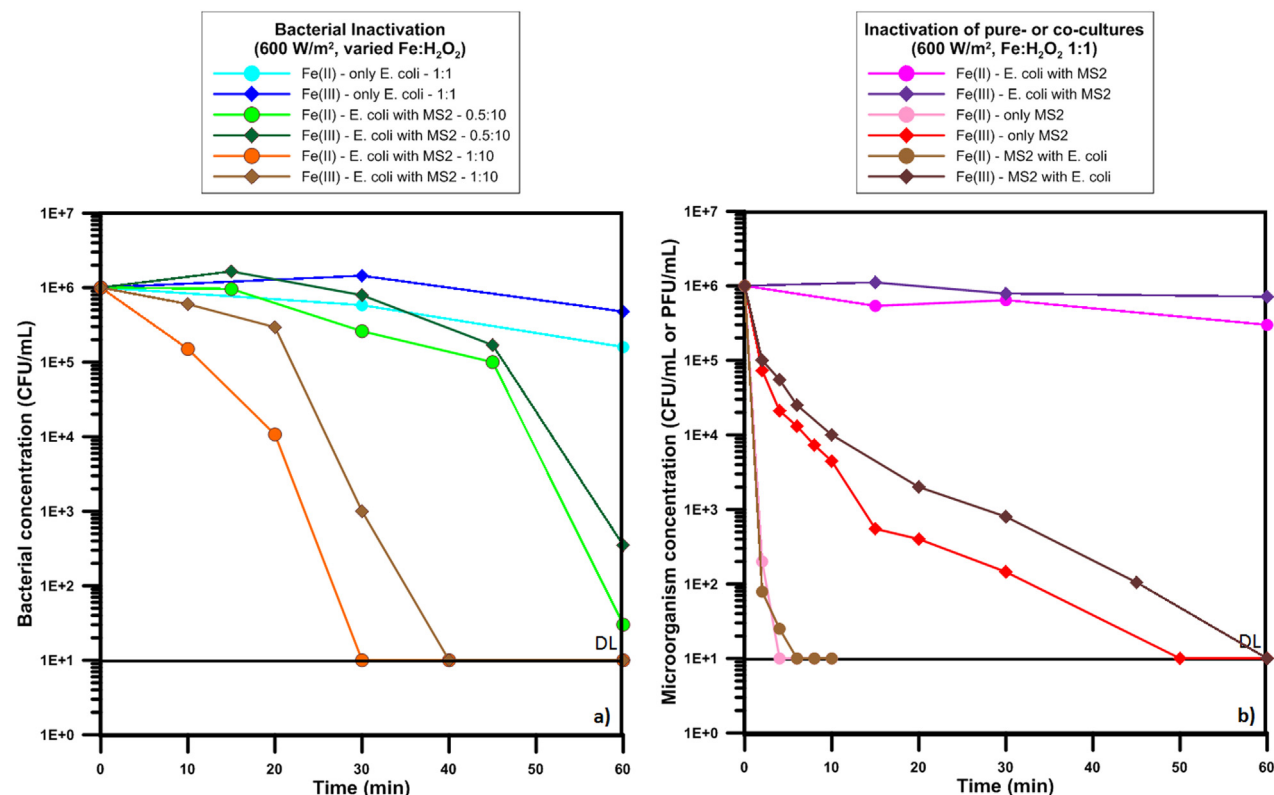

Fig. 5. Bacterial competition tests: Inactivation of MS2 and E. coli by the photo-Fenton process. a) Bacterial inactivation with increasing Fe:H$_2$O$_2$ ratios, in absence or presence of MS2. b) E. coli inactivation in presence of MS2 and MS2 inactivation in presence or absence of the bacterial host (Fe:H$_2$O$_2$ ratio 1:1). Higher Fenton reagents addition than 1:1 resulted in <2-min inactivation.

requires multiple ROS hits to damage a single cell, and is subjected to endogenous inactivation events. Even among virus strains, the ones with thinner capsids are more susceptible to inactivation by ROS [2], therefore the analogy with bacteria is compelling. In both
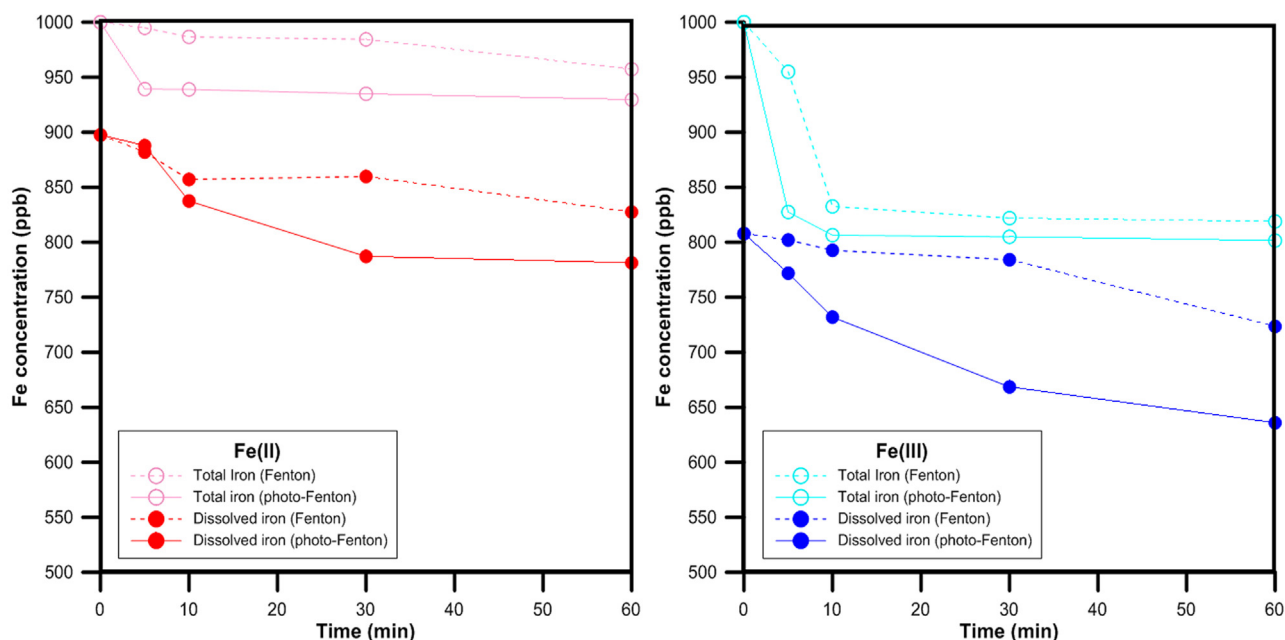
Fig. 6. Iron evolution during (dark) Fenton or photo-Fenton process followed by ICP-MS analysis (light intensity: 300 W/m^2). A) Fe(II) starting salts. B) Fe(III) starting salts. The dashed lines indicate the dark Fenton experiments, closed trace symbols indicate dissolved iron and open trace symbols the total iron.

Fig. 6a and b, Fe(II) was again proven to contribute significantly to bacterial inactivation when MS2 were absent. A noteworthy change was observed when MS2 were present in the solution, lowering the already small bacterial inactivation with the same reagent concentration. This difference is mitigated when higher reactants' addition was assayed (0.5:10 and 1:10 in mg/L ratios).

Finally, Fig. 6b demonstrates the effect the bacterial presence has on MS2 inactivation. The time necessary for total inactivation was prolonged from 5 to 10 min for MS2 with the presence of E. coli, since viruses and bacteria are in competition by the generated ROS in the system. Under the condition of steady stirring, the microbes were homogenously distributed in the water matrix and had random contacts with systemic ROS. Nevertheless, the viruses could still be totally inactivated in a short period. Furthermore, in this experiment, 1 mg/L of Fe(II) and 1 mg/L of H$_2$O$_2$ were introduced into the tested system and the simulated irradiance was set at 600 W/m^2. Recent disinfection approaches [16,20] of Fenton reagents application in the micro- to milli-molar range have been reported so far, while [15] and [38] observed the efficiency of bacterial inactivation at neutral pH by 0.6 mg/L Fe(II) or Fe(III) and 10 mg/L of H$_2$O$_2$ under 550 W/m^2 of solar radiation. Based on the results above, it can be assumed that a general dose of the Fenton reagents and sunlight exposure for bacterial disinfection is also sufficient for a fast viral inactivation in the wastewater matrix.

3.4. Iron cations solubility in wastewater

Normally, effluents that have been subjected to a biological (or other secondary) treatment, are good candidates for applying AOPs, such as the photo-Fenton process. Nevertheless, there are some characteristics that often hinder the process, such as the presence of organic matter, the alkalinity, the suspended solids and the quasi-neutral pH, among others. However, the organic matter is often considered acting in a dual manner, with capabilities of complexing metals not only antagonizing the process, but also able to facilitate the photo-Fenton process [11,12].

Similarly, the simulated wastewater used in this study was adjusted to neutral pH, at which normally iron precipitates. We studied the evolution of the photo-Fenton process, in presence of MS2 and Fe(II) or Fe(III), comparing Milli-Q (MQ) water with the studied wastewater. Over the course of two hours, there is a slight decrease in the UV–vis absorbance of the bulk in each of the iron additions in MQ (see Supplementary Fig. 2). The reference absorbance belongs to MQ water and 1, 2 and 5 mg/L of Fe(III) were added for further analyses. Additionally, WW forms more photo-absorbing, and therefore, photo-active complexes. During a 2-h test, there was practically no decrease in the absorbance, indicating the stability of the Fe-DOM complexes.

In order to verify the observations, a similar test was performed for 1 h in WW, with 1 mg/L of either Fe(II) or Fe(III). The goal of the test was to dissociate the dissolved and total iron (by 0.2 μm filtering) during an experiment at pH 7 in presence or absence of light. The main two general trends can be summarized in Fig. 6 under the higher values of dissolved iron of Fe(II) (Fig. 6a) than Fe(III) (Fig. 6b) as starting iron species, and the slightly lower precipitation rates in the dark tests. On one hand, Fe(II) readily reacts with the H$_2$O$_2$ in the matrix and then passes to Fe(III), which precipitates faster in near-neutral values, hence the fast losses in total iron presented with Fe(III) as starting iron species. The presence of organic matter helps complex the iron, efficiently perform an LMCT, and then possibly re-complex the iron. This could possibly explain the high iron availability during the tests. Finally, TOC measurements (data not shown) verify the degradation of the organic matter, however in negligible rates when low Fenton reagents' concentration was used. In conclusion, iron, even at small amounts is available to react and plays an important role in the MS2 inactivation in wastewater.

3.5. MS2 inactivation modeling

Various kinetic models have been proposed in the literature for bacterial [39] or viral inactivation [40]. According to Hiatt [41], the virus survival data can be plotted as $\ln c/c_0$ vs. $\ln t$, obtaining straight lines which are curvilinear for $\ln c/c_0$ vs. $\ln t$. Here c/c_0 is the reduction in the infective MS2 concentration and t refers to the treatment time.

Thus, the relationship between c/c_0 and t is described as the following function:

$$ln\frac{c}{c_0} = -k_{obs} \quad \ln(t+1) \tag{17}$$

where k_{obs} behaves as the observed "relative velocity constant", corresponding to a pseudo-first-order kinetic. This model was applied to fit experimental data of the photo-Fenton inactivation at pH 7 under different conditions (Table 2 and 3).

However, as seen in before, the curves of MS2 photo-inactivation with Fe(II) and H_2O_2 proceeded a sudden decrease at the very beginning of the whole process, and then changed to a tailing pattern if MS2 had not been totally inactivated. These "biphasic" survival curves can be drawn as two linear components [41,42]:

$$\text{The first stage}: \quad ln\frac{c}{c_0} = -k_{obs} \quad 1n(t+1) \tag{18}$$

$$\text{The second stage}: \quad ln\frac{c}{c_0} = -k_{obs} \quad 1n(t+1) + m \tag{19}$$

where m is the intercept of the second function on the y-axis.

For different iron starting species of Fe(II) and Fe(III), k_{light} can be determined from the slopes of k_{obs} vs. [intensity].

Ultimately, the three investigated parameters – light intensity, Fe(III) and H_2O_2 concentrations – can be linked together as a single function, within the boundaries of the experimental space, i.e. Intensity $[I] = 300–900\,W/m^2$, $[Fe(III)]_{ini} = 0.25–1\,mg/L$, $[H_2O_2]_{ini} = 0.5–1\,mg/L$), solving the Eqs. (18)-(19):

$$k_{obs} = 0.0016[I] + 2.310[Fe(III)]_{ini} + 0.7996[H_2O_2]_{ini} - 1.0701, \, r^2 = 0.9969 \tag{20}$$

Here $k_{light,Fe(III)}$ corresponds to $0.0016\,m^2\,W^{-1}\,min^{-1}$, $k_{Fe(III)}$ to $2.310\,L\,mg^{-1}\,min^{-1}$ and $k_{H_2O_2}$ to $0.7996\,L\,mg^{-1}\,min^{-1}$.

As Eq. (20) shows, k_{light} and k_{Fe} can be directly applied in the multi-parameter function in Fe(III) systems. However, $k_{H_2O_2}$ in Fe(II)-induced systems cannot be calculated due to the fast inactivation and relatively long sampling time from which the obtained k_{obs} were the same. The correlation between experimental data and the function is acceptable in the majority of the sets (Tables 2 and 3). However it must be noted that during the first two minutes of the experiments, the inactivation was so fast that it was possible to have already inactivated all the viruses or entered the second phase of disinfection.

3.6. Integrated proposal for the inactivation mechanism of viruses in wastewater

Based on our experimental findings, the inactivation scheme presented in our previous work [25] and the relevant literature, a modified framework for wastewater is suggested in Fig. 7, displaying the possible pathways occurred in virus inactivation, driven by the photo-Fenton process in wastewater. This framework postulates a modified inactivation pattern in close vicinity to the virus, also suggested as a caged mechanism by previous works [24].

Concerning the MS2 inactivation (Fig. 7, events 1–6):

1. Sunlight directly affects the viral genome, decreasing its infectivity. Other direct actions involve the damages to the coat protein, as well as considerable A protein decay [43].
2. Oxidative stress exerted by H_2O_2 on the virus is not significant, due to its low oxidation potential, while under light, due to both its poor photolysis and the presence of DOM that scavenges reactive hydroxyl radicals the expected contribution is limited. Only by combination with UVA important damages have been reported [44,45].
3. Irradiation of the DOM present in WW generates a small amount of H_2O_2, O_2^-, $^1O_2$ and other ROS. The superoxide radical anion is always generated in lower steady-state concentrations than other ROS. Also, the presence of these trace metals is reported to enhance its production [46]. As it was reported, O_2^- has minor contribution in direct MS2 infectivity decrease. On the other hand, singlet oxygen significantly affects viral infectivity [14].
4. In a dark Fenton reaction, Fe(IV) species participates predominantly in the inactivation of viruses; however, an implementation of solar light greatly enhances the production of $HO^\bullet$, which is more effective in virus inactivation [24]. When high organic matter concentrations were involved in previous works, the steady state concentrations and the use of specific $HO^\bullet$ quenchers proved that the $HO^\bullet$ contribution of the bulk is low [47]. Later works based on caged mechanisms of inactivation [48,49], suggested that $HO^\bullet$ plays a role only when generated in the vicinity of the virion [24].
5. In the wastewater matrix, Fe ions form aquo-complexes by hydrolysis and organo-complexes with the DOM present. As indicated by Rose and Waite [50], the reaction rate of Fe complexes towards ROS is the same as for the free ions. The complex
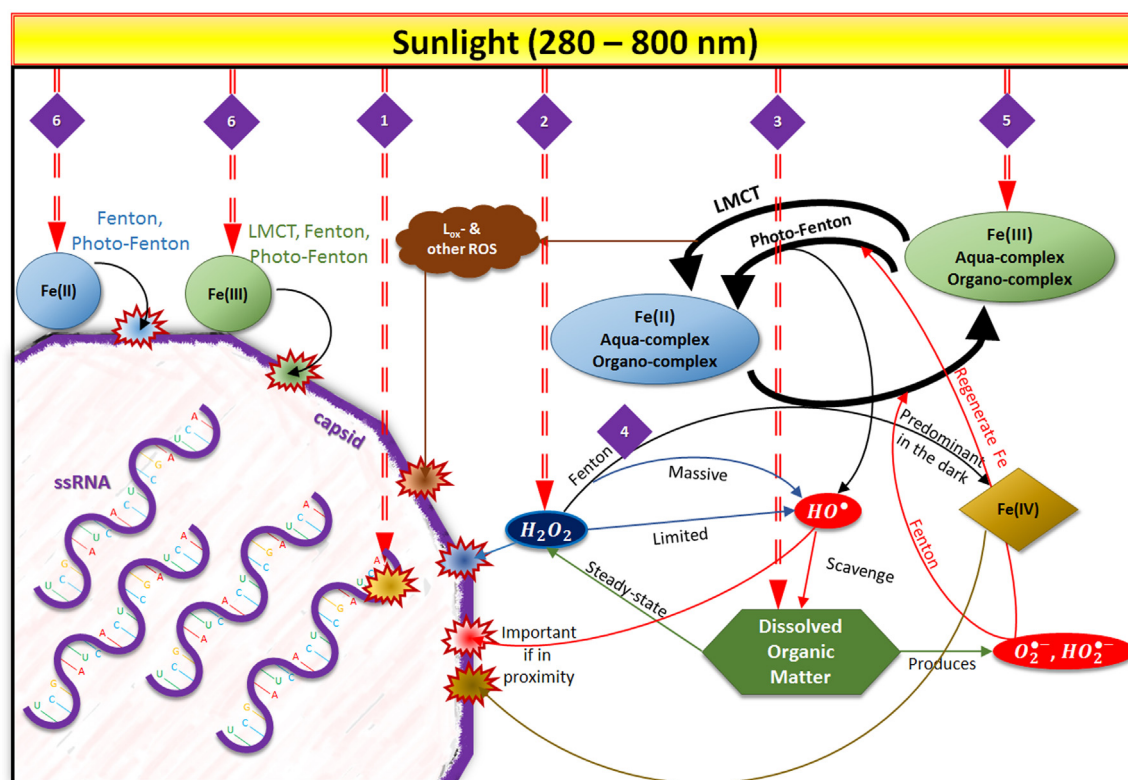
Table 2
Effect of photo-Fenton treatment [Fe(II)] on MS2 inactivation.

Light [W/m²]	Fe(II) [mg/L]	H₂O₂ [mg/L]	T₉₉.₉₉% [min]	k₁,ₒᵦₛ [min⁻¹]	r₁²	t₁ [min]	k₂,ₒᵦₛ [min⁻¹]	m	r₂²	t₂ [min]
0	0.5	1	–	2.4152	0.5770	0–5	0.3806	3.6564	0.9903	5–40
300	0.25	0.5	10	7.1218	1	0–2	1.3106	5.9716	0.9146	2–20
300	0.25	1	7.5	7.1218	1	0–2	2.3580	5.0404	0.9686	2–10
300	0.5	1	4	7.1218	1	0–2				
300	1	1	3	7.7527	1	0–2				
600	0.5	1	2	8.4208	0.9969	0–2				
600	1	1	2	20.2658	0.9986	0–0.5	2.818	7.0741	1	0.5–1
900	0.5	1	1.5	9.8486	1	0–2				

Table 3
Effect of photo-Fenton treatment [Fe(III)] on MS2 inactivation.

Light [W/m²]	Fe(III) [mg/L]	H₂O₂ [mg/L]	T₉₉.₉₉% [min]	kₒᵦₛ [min⁻¹]	r²	t [min]
0	0.5	1	–	0.1606	0.9561	0–60
300	0.25	0.5	–	0.3746	0.9142	0–30
300	0.25	1	–	0.7197	0.9094	0–60
300	0.5	1	–	1.4366	0.9653	0–40
300	1	1	33	2.4794	0.9772	0–30
600	0.5	1	32	1.8140	0.9698	0–60
900	0.5	1	30	2.2894	0.9258	0–30

Fig. 7. Proposed MS2 inactivation pathway by the photo-Fenton process in wastewater at near-neutral pH. The events 1–6 are further analyzed in the text.

formation allows the photo-Fenton reaction to proceed at neutral pH where Fe(III)-organo complexes are generally stable in particular. They show higher absorption in the visible range of solar light than aquo-complexes, favoring LMCT reaction that generates ROS under sunlight [15]. The resulting ROS (HO•, O_2^-) have been analyzed before and the oxidized ligand could possibly proceed with further ROS production [51,52].

6. Finally, Fe(II) and Fe(III) may directly interact with any of the amino acids in MS2 capsid, forming organo-complexes. In this case, the Fenton reactions can proceed on the MS2 surface [7], facilitating an LMCT reaction with the viral capsid as sacrificial ligand.

4. Conclusions

The use of μM concentrations of Fe and H_2O_2 has been proven, under certain conditions, enough to enhance the viral model inactivation in simulated wastewater. The photo-Fenton process in near-neutral conditions under the presence of scavenging DOM has proceeded to effectively reduce MS2 infectivity, and the effects of the key parameters of the process were further analyzed.

The photo-Fenton reagents' concentration was kept at ≤1 mg/L level, in order to facilitate easier kinetics studies. Even so, it proves the feasibility of removing MS2 from wastewaters. Fe(II) proven was more efficient than Fe(III), as its interaction with key components of the capsid enables the ROS production in the vicinity of the virus. Lowering the ratio among Fe:H_2O_2 (increasing iron concentration) improved the disinfection process indicating the importance of iron presence for efficient disinfection. Similar trend was observed for the pH, which improves iron solubility and therefore its participation to the photo-Fenton process. Nevertheless, the most important contribution derives from the DOM complexation of iron, which, apart from the additional ROS production, also mitigates precipitation and facilitates the maintenance of the initially

added amounts. Furthermore, a simple model describing the MS2 inactivation, including the implicated parameters, was effectively constructed.

In conclusion, we identified iron and organic matter as the key factors playing a role in the process when a complex, multi-target matrix was involved, proposing an inactivation scheme, as well as presenting the indicative difference of the needs for addition of oxidants. As in actual applications the levels of Fe and H_2O_2 addition are higher, the MS2 removal is normally expected sooner than the corresponding bacterial inactivation. Finally, further work concerning human pathogenic viral strains and other public health related microorganisms is required before establishing a relative order of removal (compared to other pathogens) and asserting the efficacy of photo-Fenton.

Appendix A. Supplementary data

Supplementary data associated with this article can be found, in the online version, at http://dx.doi.org/10.1016/j.apcatb.2016.11.034.

References

[1] K.G. McGuigan, R.M. Conroy, H.J. Mosler, M. du Preez, E. Ubomba-Jaswa, P. Fernandez-Ibanez, J. Hazard. Mater. 235–236 (2012) 29–46.

[2] A. Carratalà, A.D. Calado, M.J. Mattle, R. Meierhofer, S. Luzi, T. Kohn, Appl. Environ. Microbiol. 82 (2016) 279–288.
[3] C.V. Chrysikopoulos, I.D. Manariotis, V.I. Syngouna, Colloids and surfaces. B Biointerfaces 107 (2013) 174–179.
[4] H. Gómez-Couso, F. Méndez-Hermida, J.A. Castro-Hermida, E. Ares-Mazás, Vet. Parasitol. 133 (2005) 13–18.
[5] S.C. Weir, N.J. Pokorny, R.A. Carreno, J.T. Trevors, H. Lee, Appl. Environ. Microbiol. 68 (2002) 2576–2579.
[6] S. Malato, P. Fernández-Ibáñez, M.I. Maldonado, J. Blanco, W. Gernjak, Catal. Today 147 (2009) 1–59.
[7] J.Y. Kim, C. Lee, D.L. Sedlak, J. Yoon, K.L. Nelson, Water Res. 44 (2010) 2647–2653.
[8] S. Giannakis, C. Ruales-Lonfat, S. Rtimi, S. Thabet, P. Cotton, C. Pulgarin, Appl. Catal. B: Environ. 185 (2016) 150–162.
[9] P. Karaolia, I. Michael, I. García-Fernández, A. Agüera, S. Malato, P. Fernández-Ibáñez, D. Fatta-Kassinos, Sci. Total Environ. 468 (2014) 19–27.
[10] C. Pulgarin, CHIMIA Int. J. Chem. 69 (2015) 7–9.
[11] S. Giannakis, M.I.P. López, D. Spuhler, J.A.S. Pérez, P.F. Ibáñez, C. Pulgarin, Appl. Catal. B: Environ. 198 (2016) 431–446.
[12] S. Giannakis, M.I. Polo López, D. Spuhler, J.A. Sánchez Pérez, P. Fernández Ibáñez, C. Pulgarin, Appl. Catal. B: Environ. 199 (2016) 199–223.
[13] A.-G. Rincón, C. Pulgarin, Appl. Catal. B: Environ. 49 (2004) 99–112.
[14] T. Kohn, K.L. Nelson, Environ. Sci. Technol. 41 (2007) 192–197.
[15] D. Spuhler, J.A. Rengifo-Herrera, C. Pulgarin, Appl. Catal. B: Environ. 96 (2010) 126–141.
[16] C. Ruales-Lonfat, J.F. Barona, A. Sienkiewicz, M. Bensimon, J. Vélez-Colmenares, N. Benítez, C. Pulgarín, Appl. Catal. B: Environ. 166–167 (2015) 497–508.
[17] J.J. Pignatello, E. Oliveros, A. MacKay, Crit. Rev. Environ. Sci. Technol. 36 (2006) 1–84.
[18] J. Ndounla, S. Kenfack, J. Wéthé, C. Pulgarin, Appl. Catal. B: Environ. 148–149 (2014) 144–153.
[19] J. Ndounla, D. Spuhler, S. Kenfack, J. Wéthé, C. Pulgarin, Appl. Catal. B: Environ. 129 (2013) 309–317.
[20] E. Ortega-Gómez, M.M. Ballesteros Martín, B. Esteban García, J.A. Sánchez Pérez, P. Fernández Ibáñez, Appl. Catal. B: Environ. 148–149 (2014) 484–489.
[21] E. Ortega-Gomez, P. Fernandez-Ibanez, M.M. Ballesteros Martin, M.I. Polo-Lopez, B. Esteban Garcia, J.A. Sanchez Perez, Water Res. 46 (2012) 6154–6162.
[22] S. Giannakis, S. Papoutsakis, E. Darakas, A. Escalas-Cañellas, C. Pétrier, C. Pulgarin, Ultrason. Sonochem. 22 (2015) 515–526.
[23] J.I. Nieto-Juarez, T. Kohn, Photochem. Photobiol. Sci. 12 (2013) 1596–1605.
[24] J.I. Nieto-Juarez, K. Pierzchła, A. Sienkiewicz, T. Kohn, Environ. Sci. Technol. 44 (2010) 3351–3356.
[25] E. Ortega-Gómez, M.M. Ballesteros Martín, A. Carratalà, P. Fernández Ibañez, J.A. Sánchez Pérez, C. Pulgarín, Appl. Catal. B: Environ. 174–175 (2015) 395–402.
[26] D.A. Kuzmanovic, I. Elashvili, C. Wick, C. O'Connell, S. Krueger, J. Mol. Biol. 355 (2006) 1095–1111.
[27] M. Templeton, R. Andrews, R. Hofmann, J. Appl. Microbiol. 101 (2006) 732–741.
[28] I. Bradley, A. Straub, P. Maraccini, S. Markazi, T.H. Nguyen, Water Res. 45 (2011) 4501–4510.
[29] S. Muthukumaran, D.A. Nguyen, K. Baskaran, Desalination 279 (2011) 383–389.
[30] E. Viollier, P.W. Inglett, K. Hunter, A.N. Roychoudhury, P. Van Cappellen, Appl. Geochem. 15 (2000) 785–790.
[31] G. Eisenberg, Ind. Eng. Chem. Anal. Ed. 15 (1943) 327–328.
[32] S. Giannakis, E. Darakas, A. Escalas-Cañellas, C. Pulgarin, Chem. Eng. J. 281 (2015) 588–598.
[33] S. Giannakis, A.I. Merino Gamo, E. Darakas, A. Escalas-Cañellas, C. Pulgarin, Chem. Eng. J. 253 (2014) 366–376.
[34] P. Westerhoff, G. Aiken, G. Amy, J. Debroux, Water Res. 33 (1999) 2265–2276.
[35] E. Timchak, V. Gitis, Chem. Eng. J. 192 (2012) 164–170.
[36] R. Olsthoorn, J. Van Duin, Proc. Natl. Acad. Sci. 93 (1996) 12256–12261.
[37] M.J. Mattle, T. Kohn, Environ. Sci. Technol. 46 (2012) 10022–10030.
[38] S. Giannakis, M. Voumard, D. Grandjean, A. Magnet, L.F. De Alencastro, C. Pulgarin, Water Res. 102 (2016) 505–515.
[39] J. Marugán, R. van Grieken, C. Sordo, C. Cruz, Appl. Catal. B: Environ. 82 (2008) 27–36.
[40] C.V. Chrysikopoulos, A.F. Aravantinou, J. Hazard. Mater. 233-234 (2012) 148–157.
[41] C. Hiatt, Bacteriol. Rev. 28 (1964) 150.
[42] S. Kamolsiripichaiporn, S. Subharat, R. Udon, P. Thongtha, S. Nuanualsuwan, Appl. Environ. Microbiol. 73 (2007) 7177–7184.
[43] K.R. Wigginton, B.M. Pecson, T.r. Sigstam, F. Bosshard, T. Kohn, Environ. Sci. Technol. 46 (2012) 12069–12078.
[44] C.D. Nelson, E. Minkkinen, M. Bergkvist, K. Hoelzer, M. Fisher, B. Bothner, C.R. Parrish, J. Virol. 82 (2008) 10397–10407.
[45] O.C. Romero, A.P. Straub, T. Kohn, T.H. Nguyen, Environ. Sci. Technol. 45 (2011) 10385–10393.
[46] B.M. Voelker, D.L. Sedlak, Mar. Chem. 50 (1995) 93–102.
[47] T. Kohn, M. Grandbois, K. McNeill, K.L. Nelson, Environ. Sci. Technol. 41 (2007) 4626–4632.
[48] M. Chevion, Free Radic. Biol. Med. 5 (1988) 27–37.
[49] T. Kocha, M. Yamaguchi, H. Ohtaki, T. Fukuda, T. Aoyagi, Biochim. Biophys. Acta (BBA) Protein Struct. Mol. Enzymol. 1337 (1997) 319–326.
[50] A.L. Rose, T.D. Waite, Environ. Sci. Technol. 36 (2002) 433–444.
[51] P. Cieśla, P. Kocot, P. Mytych, Z. Stasicka, J. Mol. Catal. A: Chem. 224 (2004) 17–33.
[52] J. Šima, J. Makáňová, Coord. Chem. Rev. 160 (1997) 161–189.